Uchiyama, Ichiro; Maruoka, Akira; Kawahara, Mutsuto

Finite Element Analysis Using Stabilized Acoustic Velocity Model

12th International Conference on Hydroscience & Engineering
Hydro-Science & Engineering for Environmental Resilience
November 6-10, 2016, Tainan, Taiwan.

Finite Element Analysis Using Stabilized Acoustic Velocity Model

Ichiro Uchiyama[1] *, Akira Maruoka*[2] *, Mutsuto Kawahara*[3]
1. Ocean Consultant Japan CO., LTD, Shibaura, Minato-ku
Tokyo, Japan
2. National Institute of Technology, Hachinohe College
Hachinohe City, Aomori Prefecture, Japan
3. Chuo University, Kasuga, Bunkyo-ku
Tokyo, Japan

ABSTRACT

Recently, the adiabatic flow model, which is a computational fluid dynamics (CFD) model in an adiabatic state, has been applied to solve the actual flow problem. When using finite element method for the computational fluid dynamics, the advection and pressure-induced vibration causes numerical instability. Hence, it is very effective to apply stabilized methods to the flow model to reduce the instability. In this paper, we present the new stream-upwind/Petrov-Garelkin (SUPG) formulations of the adiabatic flow model, which include not only the effects of SUPG but also those of pressure-stabilizing/Petrov-Garelkin (PSPG) and least-square on incompressible constraint (LSIC). By employing these methods, we were able to considerably improve the stability and accuracy of computations for two dimensional cavity flows. Furthermore, we applied arbitrary Lagrangian-Eulerian (ALE) methods to solitary wave propagation. Based on these case studies, we have verified the effectiveness of our present CFD model.

KEY WORDS: Adiabatic flow model, Solitary wave propagation, Cavity flow, SUPG, PSPG, LSIC, ALE

INTRODUCTION

Numerical computations of fluid flows are usually carried out under the assumption of either incompressibility or compressibility. Formulation of an incompressibility model can be introduced when the acoustic velocity tends to infinity. However, the acoustic velocities of natural fluids are not infinite, although its values are very large in comparison with other variables. Thus, we adopted the adiabatic flow model, which is considered to have slight compressibility. In the adiabatic flow model, by assuming the adiabatic state of the fluid, the density can be expressed only as a function of the pressure. Furthermore, the assumptions of the adiabatic flows are categorized into two methods. In one method, velocity, pressure, and density are used as the working variables and density is explicitly related to pressure by using the equation of states (Terachi and Kawahara [2010], Okumura et al. [2013], Kawahara [2016], etc.). In the other method, velocity and pressure are used as the working variables, by assuming the acoustic velocity to be constant (Kawahara and Hirano [1983], Kawahara and Miwa [1983], Uchiyama and Kawahara [2015], Kawahara [2016], etc.). The latter method is known as the acoustic velocity method.

Many techniques have been proposed for the stabilized methods. When the finite element method is used, in order to reduce the instability due to the advection or pressure-induced vibration, stabilized methods such as stream-upwind/Petrov-Garelkin (SUPG) method, pressure-stabilizing/Petrov-Garelkin (PSPG) method or bubble function method are widely used. In this paper, we clarify the effectiveness of the acoustic velocity model by considering SUPG terms, PSPG terms and least-square on incompressible constraint (LSIC) terms. Furthermore, we applied arbitrary Lagrangian-Eulerian (ALE) methods for moving meshes. In the test studies of two-dimensional cavity flows, two-dimensional solitary wave propagation, and three-dimensional solitary wave propagation, the stability and accuracy of computations are considerably improved with the use of these stabilized methods. By carrying out these test studies, we can confirm the applicability of our CFD model to the fluid flow analysis in various problems and the applicability of structurally resistive design against wave action in coastal facilities.

BASIC EQUATIONS OF THE ACOUSTIC VELOCITY MODELS

The basic equations of mass and momentum are expressed as follows by considering the change in density.

$$\dot{\rho} + v_i \rho_{,i} + \rho v_{i,i} = 0 \tag{1}$$

$$\rho\left(\dot{v}_i + v_j v_{i,j}\right) + p_{,i} - \tau_{ij,j} - \rho f_i = 0 \tag{2}$$

where p, u, and v are the density, pressure and velocity, respectively, and τ_{ij} and f_i denote the total stress and body force, respectively. Since the acoustic velocity c can be expressed as Eq. 3, Eq. 1 can be transformed into Eq. 4.

$$c^2 = \frac{\partial p}{\partial \rho} \tag{3}$$

$$\dot{p} + v_i p_{,i} + \rho c^2 v_{i,i} = 0 \tag{4}$$

Finally, the following equations of mass and momentum can be derived.

$$\mathrm{A} = \phi(\dot{p} + v_i p_{,i}) + v_{i,i} = 0 \tag{5}$$

$$B_i = \rho\left(\dot{v}_i + v_j v_{i,j}\right) + p_{,i} - \tau_{ij,j} - \rho f_i = 0 \tag{6}$$

where

$$\phi = {}^{1}/_{\rho c^2} = 1/\kappa \tag{7}$$

which is the inverse of the bulk modulus κ. In many cases, the acoustic velocity c remains constant. If the acoustic velocity c tends to infinity in Eq. 5, it corresponds to the mass of incompressible flow. However, we would like to emphasize that the acoustic velocity is not infinite in natural fluids.

FINITE ELEMENT EQUATIONS

The weighted residual equation with SUPG is formulated as follows.

$$\int_v (\widetilde{p^*}A + \widetilde{v_i^*}B_i) = 0 \tag{8}$$

where $\widetilde{p^*}$and $\widetilde{v_i^*}$ are the weighting functions in SUPG and could be expressed as follows.

$$(\widetilde{p^*}\ \widetilde{v_i^*}) = (p^* v_i^*) + \tau_M (p^* v_i^*)_{,k} \begin{pmatrix} \phi v_k & \delta_{ik} \\ \delta_{jk} & \rho v_k \delta_{ij} \end{pmatrix} \begin{pmatrix} \rho\|v\|^2 & \\ & {}^{1}/_{\rho} \end{pmatrix} \tag{9}$$

On substituting Eq. 5 and Eq. 6 into Eq. 8, and by using weighting functions in Eq. 9, finite element equations could be derived as follows.

$$\begin{aligned} &\phi \int_v (p^* \dot{p}) dv + \phi \int_v (p^* v_i p_{,i}) dv + \int_v (p^* v_{i,i}) dv + \\ &\nu_A \phi^2 \int_v (p_{,i}^* v_i \dot{p}) dv + \nu_A \phi^2 \int_v (p_{,i}^* v_i v_j p_{,j}) dv + \\ &\nu_A \phi \int_v (p_{,i}^* v_i v_{j,j}) dv + \tau_p \rho \int_v (p_{,i}^* \dot{v}_i) dv + \\ &\tau_p \rho \int_v (p_{,i}^* v_i v_{i,j}) dv + \tau_p \int_v (p_{,i}^* p_{,i}) dv = 0 \end{aligned} \tag{10}$$

$$\begin{aligned} &\rho \int_v (v_i^* \dot{v}_i) dv + \rho \int_v (v_i^* v_j v_{i,j}) dv - \int_v (v_{i,i}^* p) dv + \\ &\int_v (v_{i,j}^* \tau_{ij}) dv + \nu_c \phi \int_v (v_{i,i}^* \dot{p}) dv + \nu_c \phi \int_v (v_{i,i}^* v_j p_{,j}) dv + \\ &\nu_c \phi \int_v (v_{i,i}^* v_{i,j}) dv + \tau_M \rho \int_v (v_{i,j}^* v_j \dot{v}_i) dv + \\ &\tau_M \rho \int_v (v_{i,j}^* v_j v_k v_{i,k}) dv + \tau_M \int_v (v_{i,j}^* v_j p_{,j}) dv = \\ &\int_s (v_i^* t_i) ds + \rho \int_v (v_i^* f_i) ds \end{aligned} \tag{11}$$

Where

$$\begin{aligned} \nu_A &= \rho\|v\|^2 \tau_M \\ \nu_C &= \rho\|v\|^2 \tau_M \\ \tau_p &= \frac{1}{\rho}\tau_M \end{aligned} \tag{12}$$

On the left-hand side of Eq.10, the fourth, fifth, and sixth terms are LSIC terms, and the seventh, eighth, and ninth terms are PSPG terms. On the left-hand side of Eq.11, the fifth, sixth, and seventh terms are LSIC terms, and the eighth, ninth, and tenth terms are SUPG terms. Although the LSIC method is usually applied to incompressible models, in order to stabilize the computation, we included the LSIC method in our CFD model because the fluid should be almost incompressible. In Eq.12, ν_A, ν_C, τ_p, and τ_M are the coefficients defined by Tezduyar et al [2003].

CAVITY FLOWS

In order to demonstrate the applicability of this CFD model, we have carried out the computation of the cavity flow problem. This computation is based on spatial domains that are not required to move the nodes or deform the meshes. Fig. 1 shows the computational finite element mesh. The number of nodes and meshes are 6,561 and 128,000, respectively. The boundary conditions on the right, left, and down sides are non-slip conditions, and we set the velocity to 1m/s on the upper boundary.

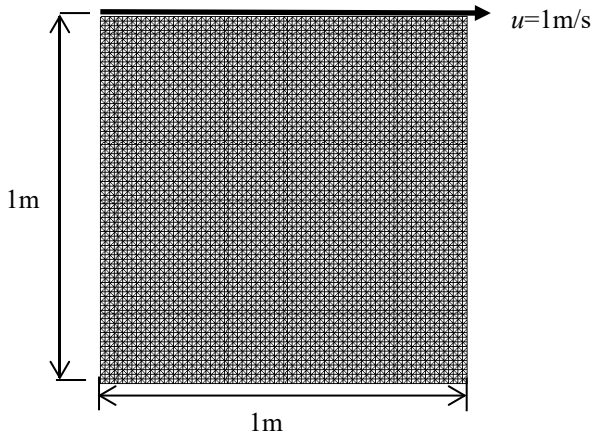

Fig. 1 Finite element meshes for the cavity flows

Fig. 2 shows the computational results of the velocity along the central axis compared with Giha's results [Ghia et al, 1982], and Fig. 3 shows the velocity distribution at the time step of 200s. In Fig. 2, each computational result corresponds with Giha's results very well. According to these computational results, our CFD model is able to provide accurate results with an incompressible flow model.

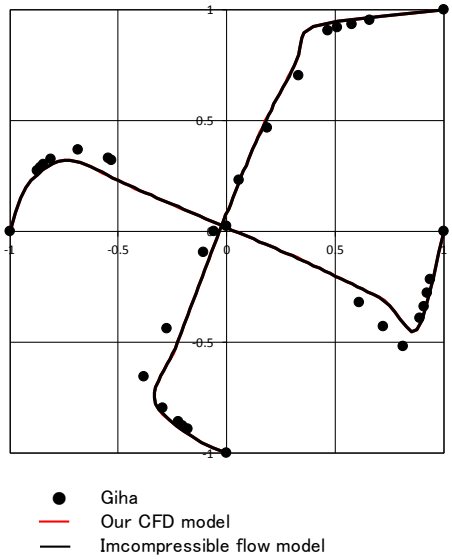

Fig. 2 Velocity along the central axis compared with Giha's results

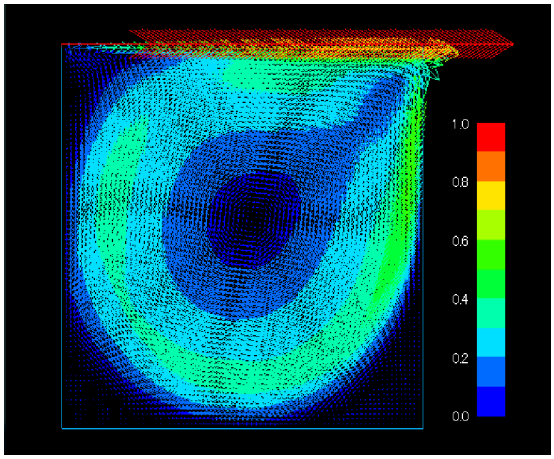

Fig. 3 Velocity distribution (Re = 1,000, T = 200 s)

TWO-DIMENSIONAL SOLITARY WAVE

We then carried out the computation of the solitary wave propagation in order to demonstrate the applicability of this CFD model. In this problem, we have to cope with the free surface condition. The mesh needs to be updated as the flow evolves. Fig.4 shows the computational finite element mesh. The number of nodes and meshes were 5,511 and 10,000, respectively. The boundary conditions on the left, right, and down sides are slip wall conditions. The initial conditions of the wave level and velocity were derived using Laitone's formula. Furthermore, we set the wave height ratio at 0.1 by considering a non-breaking wave condition.

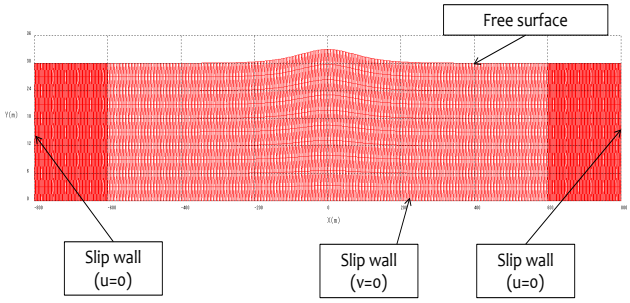

Fig. 4 Finite element meshes for two-dimensional solitary wave propagation

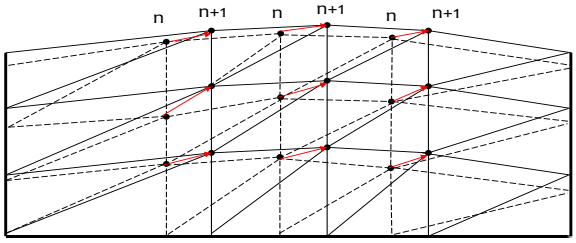

Free surface treatment

$$x^{n+1} = x^n + u^n \cdot \Delta t$$
$$y^{n+1} = y^n + v^n \cdot \Delta t$$

Fig. 5 Schematic expression of ALE method

In this computation, we applied the ALE method to the flow to avoid having to collapse the meshes. Fig. 5 shows the schematic expression of the ALE method. Nodes on the free surface move according to the interface-tracking techniques. In contrast, nodes in the fluid move according to the ALE approach. The x-coordinate of the nodes in the fluid invariably corresponds to those on the free surface.

Fig. 6 shows the solitary wave propagation. The colors in the figure denote the pressure distribution. In these computational results, the solitary wave propagates and reflects from the wall accurately.

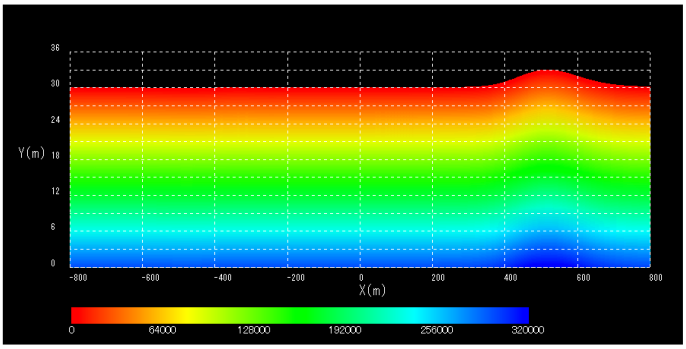

(1) T = 30 s

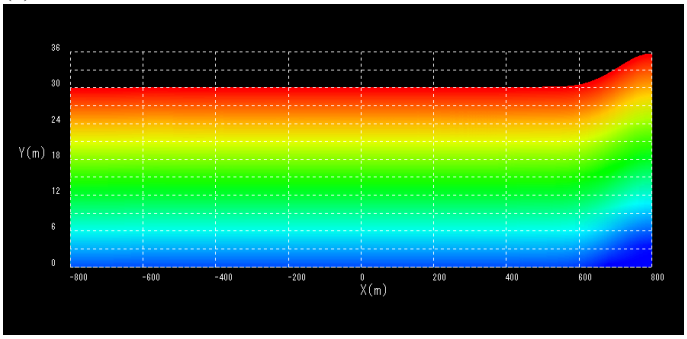

(2) T = 45 s

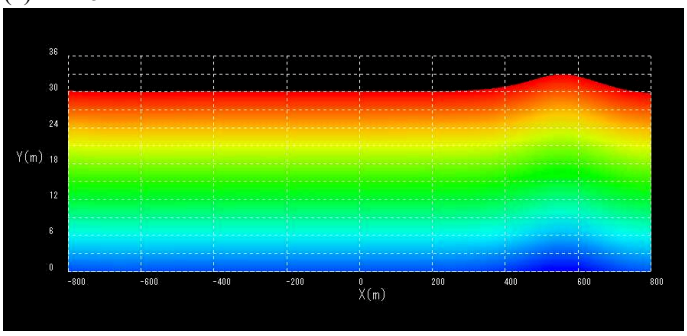

(3) T = 60s

Fig. 6 Solitary wave propagation (Two-dimensional)

THREE-DIMENSIONAL SOLITARY WAVE

We then computed the three-dimensional solitary wave propagation in order to demonstrate the applicability of this CFD model. Fig.7 shows the schematic view and the computational condition. The number of nodes and elements are 30,371 and 125,000, respectively. We set the wave height ratio at 0.12 by considering a non-breaking wave condition. We set a slope of 1/20 in the middle of the channel. The depth on the downstream side was 0.5m from the surface to the reef topography.

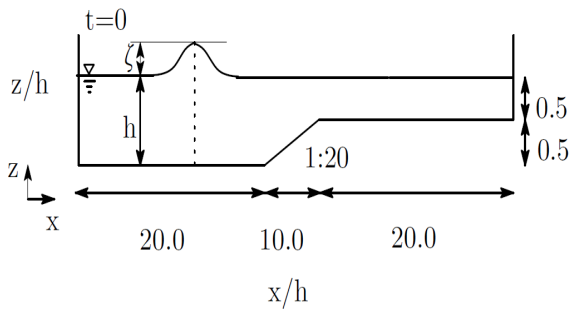

Fig. 7 Schematic view of the three-dimensional solitary wave propagation

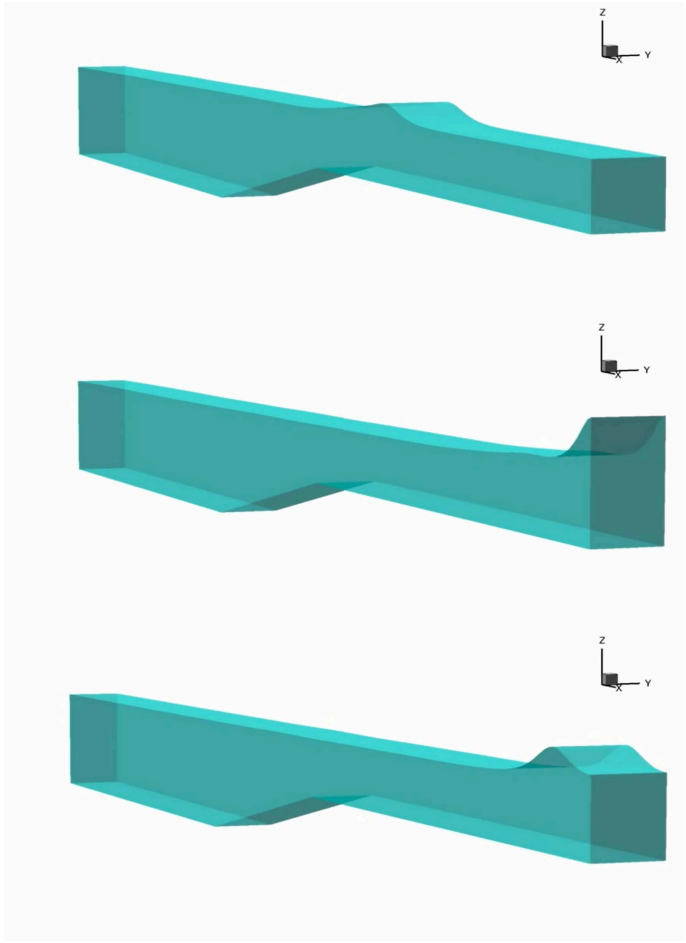

Fig. 8 Solitary wave propagation (three-dimensional)

Fig. 8 shows the solitary wave propagation. In these computational results, the solitary wave propagates on the reef and transforms itself. It reflects from the wall, while maintaining its shape.

Fig. 9 shows the computational time history of the non-dimensional water level compared with Street's results [Street et al, 1968] at x/h=41.6 on the reef topography. These computational results correspond with Street's results very well.

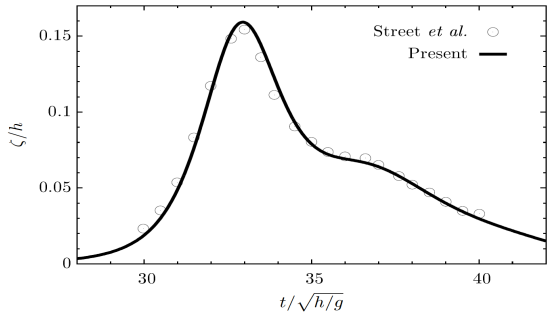

Fig. 9 Computational time history of the non-dimensional water level compared with Street's results

CONCLUSIONS

In this study, the applicability of the acoustic velocity model in both air and water was confirmed. Therefore, it is clear that this CFD model can be applied to various flow problems. However, to stabilize the computation, stabilized methods such as SUPG, PSPG, LSIC, and ALE are necessary. In the near future, we intend to apply this CFD model to structurally resistive design against wave action in the coastal facilities or the shape optimization problem of coastal facilities.

REFERENCES

M. Kawahara: Finite element method of incompressible, adiabatic, and compressible flows: From Fundamental Concepts to Applications (Mathematics for Industry), Springer, 2016.

M. Kawahara, H. Hirano: A finite element method for high Reynolds number viscous fluid flow using two step explicit scheme, International Journal for Numerical Methods in Fluid, Vol.3 (1983), 137-163.

M. Kawahara, T. Miwa: Finite element analysis of wave motion, International Journal for Numerical Methods in Engineering, Vol.20 (1984), 1193-1210.

S. Nasu, K. Nojima, M. Kawahara: SUPG finite element method for adiabatic flows, Computer and Mathematics with Application, Vol.66 (2013), 250-268.

H. Okumura, Y. Hikino, M. Kawahara: A shape optimization method of a body located in adiabatic flows, International Journal of Computational Fluid Dynamics, Vol.27 (2013), 297-306.

R.L. Street, S.L. Burges, P.W. Whitford: Dept. of Civil Engng., Stanford Univ. Tech. Rept. No.93, 1968.

K. Terachi, M. Kawahara: Shape optimization of a body located in viscous flows using the acoustic velocity method, Internal paper in Kawahara Laboratory, Chuo University.

T. E. Tezduyar and S. Sathe: Stabilaization parameter in SUPG and PSPG formulations,Journal of computational and applied mechanics, Vol.4, No.1 (2003), 71-88.

T. E. Tezduyar: Stabilized finite element formulations for incompressible flow computations, Advances in Applied Mechanics, Vol.28 (1991), 1-44.

I. Uchiyama, M. Kawahara: Finite element analysis of adiabatic flows, 13th US National Congress on Computational Mechanics, Jul. 26th-Jul. 30th, 2015, San Diego, CA.